Available online at www.sciencedirect.com
ScienceDirect
Journal of Sound and Vibration 307 (2007) 481–494
JOURNAL OF SOUND AND VIBRATION
www.elsevier.com/locate/jsvi

Modelling vibrations on deformed rolling tyres—a modal approach

I. Lopez[a,*], R.E.A. Blom[b], N.B. Roozen[a], H. Nijmeijer[a]

[a]*Section Dynamics and Control, Department of Mechanical Engineering, Eindhoven University of Technology, P.O. Box 513, 5600 MB Eindhoven, The Netherlands*
[b]*Oce Technologies B.V., St. Urbanusweg 43, 5900 MA Venlo, The Netherlands*

Received 11 April 2005; received in revised form 14 May 2007; accepted 16 May 2007
Available online 10 September 2007

Abstract

This paper examines an approach to model the vibrations of a deformed rolling tyre at low frequencies (below 500 Hz). The starting point for this approach is a finite element (FE) model of the tyre and the aim is to calculate the dynamic response of a rolling tyre including the details of its complex build up. This allows to relate the tyre design parameters to its vibro-acoustic properties. In this context, a modal approximation based on the eigenvalues and eigenvectors extracted from the detailed FE model of the tyre seems a computationally efficient possibility. In the proposed approach the natural frequencies and modeshapes of a deformed tyre are calculated in a standard FE package using the full (nonlinear) FE model. Subsequently, this modal base is transformed to determine the response of the rotating tyre in a fixed (Eulerian) reference frame. Furthermore, this approach makes it possible to define a receptance matrix for the rotating tyre. Results from relatively simple tyre models show that the effects of rotation are modelled correctly and are in accordance with results from literature.

1. Introduction

Road traffic noise is becoming an increasingly big problem in densely populated areas. This noise consists mainly of tyre/road noise and engine noise. In the past, engine noise has been the dominating noise source at most constant driving speeds, but in the past decades this balance has shifted towards tyre/road noise. At present, tyre/road noise is the dominating noise source for constant driving speeds of >40 km/h [1]. Tyre/road noise generation mechanisms are generally divided in two main groups [2]: vibrational mechanisms and aerodynamical mechanisms. In the dominant frequency range for exterior noise (500–2000 Hz [2]) both vibrational and aerodynamical mechanisms make significant contribution [2,3]. For the interior noise in a car, to which the occupants of the vehicle are exposed, tyre/road noise is also an important source, especially at lower frequencies. Tyre vibrations (up to approximately 500 Hz [2]) induce forces on the hub which are transmitted via the suspension and the car structure to the interior, thus significantly contributing to the

*Corresponding author. Tel.: +31 40 247 2611; fax: +31 40 246 1418.
E-mail address: i.lopez@tue.nl (I. Lopez).

0022-460X/$ - see front matter © 2007 Elsevier Ltd. All rights reserved.
doi:10.1016/j.jsv.2007.05.056

interior noise. The hub forces are caused by two main phenomena: belt vibrations excited by the tyre/road contact and acoustic resonances of the air column inside the tyre, also known as cavity modes [2]. In the present paper, only tyre vibrations are considered and the wheel is assumed infinitely stiff. However, the proposed methodology can also be applied to a model including the wheel compliance and the acoustic cavity in the tyre.

A number of analytical models have been proposed in the literature to model tyre vibrations. They can be mainly categorized into ring models (variations across the width direction are not included) [4–6], plate models (where the tyre curvature is neglected) [5,7–10] and cylindrical shell models [11–15]. Although the above-mentioned models differ in complexity and applicability range, they all have in common that tyre dynamics are captured in a few model parameters which can be obtained from measurements. Although analytical models have proved to be valuable to study the general dynamic behavior of tyres, they are difficult to use in the tyre design process. Recently, a promising approach referred to as Waveguide Finite Elements has been proposed [16], where the cross-section of the tyre is modelled using finite element (FE) and the vibration field in the circumferential direction is represented using waveguides.

In most of the above works the response of the tyre is determined in the tyre reference frame and the rotation is included by letting the load travel along the tread. In the more recent publications, the tyre response is either determined in a fixed-reference frame [13] or transformed from the tyre reference frame to the fixed frame [14,10]. The conclusion is that in the fixed-reference frame the main influence of the rotation is a kinematic shift of the dispersion curves which depends on the rotational velocity.

Regarding the application of the finite-element method (FEM) to tyres, only works where a modal approach is used and/or the rotation of the tyre is considered will be mentioned here. Ref. [17] Chang and Yang use a modal approach based on a FE model of a tyre to determine the response to a rotating load. They show that resonances occur at frequencies different from the natural frequencies of the non-rotating tyre. However no results regarding the response of the rotating tyre are shown. Furthermore the deformation of the tyre due to ground contact is not taken into account.

In Ref. [18], Thompson discusses the influence of rotation on the dynamic response of train wheels using a modal approach. He calculates the natural frequencies and modeshapes of the wheel using a FE model, which allows to model the wheel in great detail without having to cope with excessive simulation times. He concludes that due to the rotation a splitting of the eigenvalues occurs. Thompson determines the response of the rotating wheel in a non-rotating reference frame, which allows to use the computed vibration velocities directly in a sound radiation analysis. However in this model the deformation of the wheel due to the ground contact is not taken into account, which is acceptable for train wheels but not for tyres.

In a recent publication Brinkmeier et al. [19] used the arbitrary Lagrange–Eulerian (ALE) formulation [20] to determine the eigenvalues and modes of a stationary rolling tyre in ground contact, conclusions are similar to those of Kim and Bolton [13]. Unfortunately, only limited results are derived. Main drawback of this approach is that a special FE code is required for the ALE formulation, which is not included in standard FE packages.

The present paper deals with a new approach to model the vibration response of a rolling tyre based on a FE model of the tyre. Using a detailed FE model of a tyre is a feasible approach in the lower-frequency range (dominant region for interior noise) that makes it possible to relate tyre design parameters to its vibro-acoustic properties. Although the proposed methodology can also be applied to a FE model including the wheel compliance and the acoustic cavity in the tyre, in this first step only tyre vibrations are considered and the wheel is assumed infinitely stiff. The approach presented in this paper can be summarised as follows:

- A modal approach is used, based on modal information extracted from a FE calculation. In this way, it is possible to model the complex build-up of the tyre in detail.
- The natural frequencies and mode shapes of a deformed non-rotating tyre are calculated using a standard FE package. Therefore, the influence of the ground contact on the dynamic properties of the tyre is taken into account.
- The influence of the rotation is taken into account using a coordinate transformation. As a consequence the stiffening of the tyre due to the centrifugal forces and the Coriolis effect are included in the model.

- The response of the rotating tyre is determined in non-rotating (Eulerian) coordinates. This means that a receptance matrix of the rotating tyre can be determined in a straight forward manner.

The present paper is organized as follows: in Section 2 previous work on the effect of rotation on tyre dynamics is discussed. Then in Section 3 the proposed approach is presented. After that, in Section 4 some results using the proposed approach are derived and compared to results from literature. Finally, the conclusions and future work are summarised.

2. Background

The influence of rotation on the dynamic response of the tyre has been widely discussed in the literature. In early works [21,22] the "bifurcation" effect on the natural frequencies of the tyre due to the Coriolis acceleration is shown. More recently, in their study of a rotating cylindrical shell, Kim and Bolton [13] conclude that for normal rotational velocities in tyres the effect of Coriolis acceleration is negligible and the main influence of rotation is a kinematic shift of the dispersion curves which can be described with the following equation:

$$f = f_s \pm \frac{k_\phi a}{2\pi}\Omega = f_s \pm \frac{n}{2\pi}\Omega, \tag{1}$$

where f is the rotation-compensated tyre natural frequency [Hz], f_s is the stationary tyre natural frequency [Hz], k_ϕ is the wavenumber [m^{-1}], a is the tyre radius [m], Ω is the tyre rotational velocity [rad/s] and, n is the number of wavelengths along the circumference [Hz].

They propose to use Eq. (1) to transform the response of the non-rotating tyre in the wavenumber–frequency domain in order to obtain the response of the rotating tyre. This approach is also used in Ref. [10] to transform the response of the tyre determined in the tyre-reference frame to the fixed-reference frame and is referred to as Doppler shift. In Ref. [14] the Doppler shift is introduced by modifying the wave velocities in a way similar to Eq. (1).

In his work on train wheels, Thompson [18] shows that when the wheel response is viewed from a fixed-reference frame, the resonances at frequency ω_r split into two peaks at $\omega_r \pm n\Omega$, and this coincides with the result in Eq. (1). He also shows that, if the response of the wheel is determined on a non-rotating reference frame, a receptance matrix can be defined for the rotating wheel with resonances at frequencies $\omega_r \pm n\Omega$.

From the above results, it is clear that the effect of rotation cannot be neglected. As mentioned in the introduction, using a modal approach to calculate the time-domain response of a tyre may be a computationally cheap approach. However, if one simply determines the natural frequencies and modeshapes of the non-rotating tyre and then models the rotation by rotating a force around the tyre (like in Ref. [17]), the gyroscopic forces and the stiffening due to rotation are not included in the model and further the resulting response of the tyre is calculated in a rotating frame. It is often convenient to find the response of the tyre in a fixed, non-rotating reference frame, which means that a transformation from one frame to the other is needed. Thompson in Ref. [18] has performed this transformation but he works with an axisymmetric model, which has repeated eigenvalues. In this case, for each eigenfrequency, there are two eigenmodes with the same number of nodal diameters n (except for $n = 0$). The relative orientation of these two eigenmodes with respect to each other is fixed but the absolute orientation is undetermined. In Thompson's case, the transformation from rotating to fixed frame is a simple coordinate transformation, which is a good approach for train wheels. However, an important aspect of tyres is that, when loaded, there is only one eigenmode associated to a given eigenfrequency and the orientation of each eigenmode is fixed due to the deformation at the contact with the road. Therefore, the results in Ref. [18] are not directly applicable to tyres.

In Ref. [19], this is solved by using an ALE-approach (see Ref. [20]). Nackenhorst proposes a modified FE formulation of the tyre which describes the dynamics of the rotating tyre in a fixed-reference frame. The eigenvalues of the tyre are determined in a stationary rolling deformed state. Once these eigenvalues have been determined, the transient response can be determined using the modal superposition principle. The approach presented in the present paper is similar to the work in [19]. The main difference is that in the current approach

a standard FE formulation is used to find a modal base for the deformed, non-rotating tyre and the dynamic equations of the rolling tyre in the fixed-reference frame are formulated in terms of this modal base.

3. Theory

3.1. Definitions

In the following derivations, two coordinate systems are used: $\mathbf{e}_1$ and $\mathbf{e}_2$. $\mathbf{e}_1$ is the reference coordinate system that is fixed to the center of the tyre and translates together with the tyre, but does not rotate. $\mathbf{e}_2$ is a body-fixed coordinate system. This means that this system rotates along with the tyre at velocity Ω (see Fig. 1). In these systems the angles α in the body-fixed frame and β in the reference frame are defined, where a certain point k on the tyre is, $\beta_k = \alpha_k + \Omega t$.

For the rotation matrix $\mathbf{A}_{21}(t)$ defined by

$$\mathbf{A}_{21}(t) = \begin{bmatrix} \cos(\Omega t) & \sin(\Omega t) & 0 \\ -\sin(\Omega t) & \cos(\Omega t) & 0 \\ 0 & 0 & 1 \end{bmatrix}, \tag{2}$$

the following equation holds

$$\mathbf{e}_2 = \mathbf{A}_{21}\mathbf{e}_1, \tag{3}$$

where Ω is the rotational velocity of the rotating reference frame. The time derivative of the rotation matrix is given by

$$\dot{\mathbf{A}}_{21}(t) = \hat{\mathbf{\Omega}}\mathbf{A}_{21}(t), \tag{4}$$

where

$$\hat{\mathbf{\Omega}} = \begin{bmatrix} 0 & \Omega & 0 \\ -\Omega & 0 & 0 \\ 0 & 0 & 0 \end{bmatrix} \tag{5}$$

and the second derivative is given by

$$\ddot{\mathbf{A}}_{21}(t) = \hat{\mathbf{\Omega}}^2\mathbf{A}_{21}(t). \tag{6}$$

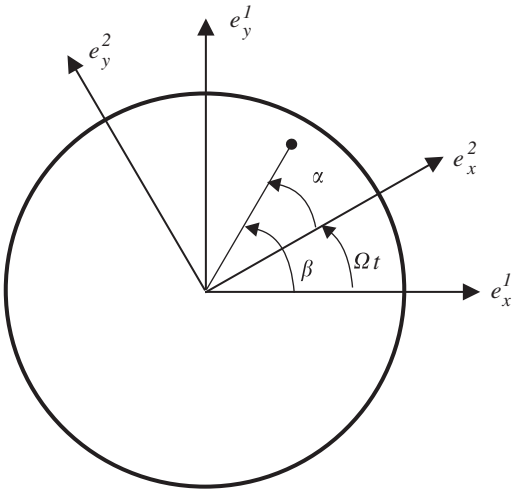

Fig. 1. The coordinate systems where $\beta = \alpha + \Omega t$.

Without loss of generality, the excitation can be defined as a point force that acts at a fixed position in the reference frame. In the reference frame $\mathbf{e}_1$, this force can be written as

$$\mathbf{f}_1^{\mathrm{T}}\mathbf{e}_1 = [F_x\delta(\beta)\ F_y\delta(\beta)\ F_z\delta(\beta)]\mathbf{e}_1, \tag{7}$$

where δ is the Dirac delta function. This leads to the following "rotating" force in the body-fixed frame:

$$\mathbf{f}_2^{\mathrm{T}}\mathbf{e}_2 = [F_x\delta(\alpha+\Omega t)\ F_y\delta(\alpha+\Omega t)\ F_z\delta(\alpha+\Omega t)]\mathbf{A}_{12}(t)\mathbf{e}_2, \tag{8}$$

where

$$\mathbf{A}_{12} = (\mathbf{A}_{21})^{-1} = (\mathbf{A}_{21})^{\mathrm{T}}. \tag{9}$$

3.2. Body-fixed-frame modes

As mentioned before for an undeformed tyre, if the stiffening due to rotation and the gyroscopic effects are neglected, the rotation may be modelled as a force which rotates around the tyre. In that case, the response of the (undamped) system can be determined from the following set of equations:

$$\mathbf{M}_2^{\mathrm{bf}}(\alpha)\ddot{\mathbf{u}}_2(t) + \mathbf{K}_2^{\mathrm{bf}}(\alpha)\mathbf{u}_2(t) = \mathbf{f}_2(\alpha+\Omega t, t), \tag{10}$$

where $\mathbf{u}_2(t)$ is the displacement column and $\mathbf{f}_2(\alpha+\Omega t, t)$ is the rotating force in $\mathbf{e}_2$. The superscript bf in Eq. (10) indicates that the body-fixed frame is considered.

Using the standard transformation to modal coordinates

$$\mathbf{u}_2^{\mathrm{bf}}(t) = \mathbf{\Phi}_2^{\mathrm{bf}}\boldsymbol{\eta}(t), \tag{11}$$

Eq. (10) can be written as

$$\ddot{\boldsymbol{\eta}}(t) + \mathbf{V}\boldsymbol{\eta}(t) = \mathbf{\Phi}_2^{\mathrm{bf}\,\mathrm{T}}\mathbf{f}_2(\alpha+\Omega t, t), \tag{12}$$

where $\mathbf{V}$ is the matrix containing the eigenvalues and $\mathbf{\Phi}_2^{\mathrm{bf}} = \mathbf{\Phi}_{\mathrm{FEM}}$ is the matrix of modal columns determined from a standard FE calculation.

This is a good approach for an unloaded tyre, where the orientation of the eigenmodes is not fixed and the position of the nodal lines is entirely determined by the choice of excitation point, but it is not appropriate to predict the response of a deformed rotating tyre. To directly determine the response of the tyre in the reference frame and be able to predict the response of a deformed rotating tyre, another approach has to be used and it is described in Section 3.3.

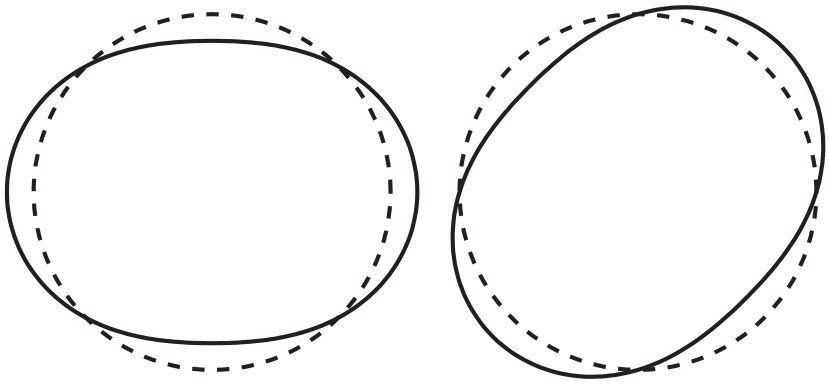

Fig. 2. Example of two degenerated modes with $n = 2$.

3.3. Reference frame-fixed modes

In the undeformed state a tyre has repeated eigenvalues and for each eigenfrequency, there are two different eigenmodes. These two eigenmodes have identical shapes, but are rotated $180/2n$ degrees with respect to each other, where n is the number of waves along the circumference, see, e.g. Fig. 2.

This means that a nodal diameter of one modeshape is an anti-nodal diameter of the other. The absolute orientation of this eigenmode pair is arbitrary and completely determined by the choice of excitation positions. When the tyre is excited by a point force the two modes of the same frequency combine in such a way that the excitation force always acts at an anti-nodal diameter.

However, when the tyre is loaded and in contact with the ground, the eigenvalues of the system are all distinct and there is only one eigenmode associated to each eigenfrequency. Furthermore, the modeshapes have a clear orientation due to the initial deformation, and the classification of modeshapes in terms of the number of nodal diameters is not straightforward. For a loaded tyre, the modeshapes are in fact fixed to the reference frame $\mathbf{e}_1$, as are the mass and stiffness matrix.

A mode $\boldsymbol{\phi}^{\mathrm{rf}}$ which is fixed to the reference frame (indicated by the subscript rf) can be described as follows:

$$\boldsymbol{\phi}^{\mathrm{rf}} = \boldsymbol{\phi}_1^{\mathrm{rf}\,\mathrm{T}}\mathbf{e}_1 = \begin{bmatrix} \phi_x(\beta) \\ \phi_y(\beta) \\ \phi_z(\beta) \end{bmatrix}^{\mathrm{T}} \mathbf{e}_1 = \begin{bmatrix} \phi_x(\alpha+\Omega t) \\ \phi_y(\alpha+\Omega t) \\ \phi_z(\alpha+\Omega t) \end{bmatrix}^{\mathrm{T}} \mathbf{A}_{12}\mathbf{e}_2. \tag{13}$$

This means that a mode which is constant in the reference frame is time dependent in the body fixed frame. The matrices $\boldsymbol{\Phi}_i^{\mathrm{rf}}$ containing m modeshapes can now be defined by

$$\boldsymbol{\Phi}_i^{\mathrm{rf}} = [\,\boldsymbol{\phi}_{i,1}^{\mathrm{rf}} \quad \cdots \quad \boldsymbol{\phi}_{i,m}^{\mathrm{rf}}\,] \quad \text{with } i = 1,2 \tag{14}$$

which for the reference coordinate system ($\mathbf{e}_1$) becomes

$$\boldsymbol{\phi}_{1,m}^{\mathrm{rf}} = \begin{bmatrix} \phi_{x,m}(\beta) \\ \phi_{y,m}(\beta) \\ \phi_{z,m}(\beta) \end{bmatrix} = \boldsymbol{\phi}_{\mathrm{FEM},m} \tag{15}$$

and for the body-fixed coordinate system ($\mathbf{e}_2$)

$$\boldsymbol{\phi}_{2,m}^{\mathrm{rf}} = \mathbf{A}_{21} \begin{bmatrix} \phi_{x,m}(\alpha+\Omega t) \\ \phi_{y,m}(\alpha+\Omega t) \\ \phi_{z,m}(\alpha+\Omega t) \end{bmatrix}. \tag{16}$$

For the mass matrix, this means

$$\mathbf{M}_1^{\mathrm{rf}}(\beta) = \mathbf{A}_{12}(\Omega t)\mathbf{M}_2^{\mathrm{rf}}(\alpha+\Omega t)\mathbf{A}_{21}(\Omega t) \tag{17}$$

and for the stiffness matrix

$$\mathbf{K}_1^{\mathrm{rf}}(\beta) = \mathbf{A}_{12}(\Omega t)\mathbf{K}_2^{\mathrm{rf}}(\alpha+\Omega t)\mathbf{A}_{21}(\Omega t). \tag{18}$$

When using reference frame-fixed modes $\mathbf{M}_1^{\mathrm{rf}}(\beta) = \mathbf{M}_{\mathrm{FEM}}$ and $\mathbf{K}_1^{\mathrm{rf}}(\beta) = \mathbf{K}_{\mathrm{FEM}}$. The equations of motion of the tyre in the body fixed, Lagrangian coordinates are given by

$$\mathbf{M}_2^{\mathrm{rf}}(\alpha+\Omega t)\ddot{\mathbf{u}}_2(t) + \mathbf{K}_2^{\mathrm{rf}}(\alpha+\Omega t)\mathbf{u}_2(t) = \mathbf{f}_2(\alpha+\Omega t, t) \tag{19}$$

The above system of equations is the same as Eq. (10) except for the mass and stiffness matrices which are now fixed to the reference frame. The variable $\mathbf{u}_2(t)$ can be transformed into the reference coordinate system by using the material derivative

$$\frac{\mathrm{D}}{\mathrm{D}t} = \frac{\partial}{\partial t} + \Omega\frac{\partial}{\partial \beta}, \tag{20}$$

where the left-hand side represents the time derivative in the body-fixed (Lagrangian) coordinates, the first term on the right-hand side is the time derivative in the reference (Eulerian) coordinates, Ω is the rotational speed and β is the circumferential angle in the reference frame. After applying Eq. (20), Eq. (19) can be expressed as

$$\mathbf{M}_2^{\mathrm{rf}} \frac{\mathrm{D}^2\mathbf{u}_2(\beta,t)}{\mathrm{D}t^2} + \mathbf{K}_2^{\mathrm{rf}}\mathbf{u}_2(\beta,t) = \mathbf{f}_2(\beta,t). \tag{21}$$

Transforming back to the reference coordinates and pre-multiplying by $\mathbf{\Phi}_1^{\mathrm{rf}}(\beta)^{\mathrm{T}}$ leads to (keeping in mind Eq. (17) and that $\mathbf{A}_{12}\hat{\mathbf{\Omega}}\mathbf{A}_{21} = \hat{\mathbf{\Omega}}$)

$$\ddot{\boldsymbol{\eta}}(t) + 2\mathbf{P}(\Omega)\dot{\boldsymbol{\eta}}(t) + (\mathbf{S}(\Omega) + \mathbf{V})\boldsymbol{\eta}(t) = \mathbf{\Phi}_1^{\mathrm{rf}^{\mathrm{T}}}(\beta)\mathbf{f}_1(t), \tag{22}$$

where

$$\mathbf{P}(\Omega) = \mathbf{\Phi}_1^{\mathrm{rf}^{\mathrm{T}}}(\beta)\mathbf{M}_1^{\mathrm{rf}}\left(\hat{\mathbf{\Omega}}\mathbf{\Phi}_1^{\mathrm{rf}}(\beta) + \Omega\frac{\partial\mathbf{\Phi}_1^{\mathrm{rf}}(\beta)}{\partial\beta}\right), \tag{23}$$

$$\mathbf{S}(\Omega) = \mathbf{\Phi}_1^{\mathrm{rf}^{\mathrm{T}}}(\beta)\mathbf{M}_1^{\mathrm{rf}}\left(\hat{\mathbf{\Omega}}^2\mathbf{\Phi}_1^{\mathrm{rf}}(\beta) + 2\Omega\hat{\mathbf{\Omega}}\frac{\partial\mathbf{\Phi}_1^{\mathrm{rf}}(\beta)}{\partial\beta} + \Omega^2\frac{\partial^2\mathbf{\Phi}_1^{\mathrm{rf}}(\beta)}{\partial\beta^2}\right) \tag{24}$$

and $\mathbf{\Phi}_1^{\mathrm{rf}}(\beta) = \mathbf{\Phi}_{\mathrm{FEM}}$ are the modeshapes determined in the FE analysis. The matrix $\mathbf{P}$ (skew-symmetric) accounts for the gyroscopic forces and the matrix $\mathbf{S}$ (symmetric) includes the stiffening effect due to rotation.

The system of equations given in Eq. (12) is an uncoupled set of equations, but this is no longer the case in Eq. (22). The matrices $\mathbf{P}$ and $\mathbf{S}$ are not diagonal, which means that Eq. (22) is a system of coupled equations. If necessary, a second eigenvalue analysis can be performed on Eq. (22) to determine the natural frequencies and modeshapes of the rotating tyre and to find a new set of uncoupled equations.

Additionally, proportional damping can be included in the formulation leading to the following system of equations (the derivation can be found in Appendix A):

$$\ddot{\boldsymbol{\eta}}(t) + (2\mathbf{P}(\Omega) + \mathbf{D}_{\mathrm{mod}})\dot{\boldsymbol{\eta}}(t) + (\mathbf{S}(\Omega) + \mathbf{D}_{\mathrm{mod}}\mathbf{P}(\Omega) + \mathbf{V})\boldsymbol{\eta}(t) = \mathbf{\Phi}_1^{\mathrm{rf}^{\mathrm{T}}}(\beta)\mathbf{f}_1(t), \tag{25}$$

where $\mathbf{D}_{\mathrm{mod}}$ is the diagonal modal damping matrix. The additional term $\mathbf{D}_{\mathrm{mod}}\mathbf{P}(\Omega)$ makes the stiffness matrix non-symmetric and contributes to the rolling resistance of the tyre [23].

The response in the reference frame can now directly be determined from

$$\mathbf{u}_1^{\mathrm{rf}}(t) = \mathbf{\Phi}_1^{\mathrm{rf}}\boldsymbol{\eta}(t). \tag{26}$$

If Eqs. (22) and (26) are transformed to the frequency domain and combined, the receptance matrix of the rotating tyre can be determined:

$$\mathbf{H}_1^{\mathrm{rf}}(\omega,\Omega) = \mathbf{\Phi}_1^{\mathrm{rf}}[-\omega^2\mathbf{I} + \mathrm{i}\omega(2\mathbf{P}(\Omega) + \mathbf{D}_{\mathrm{mod}}) + (\mathbf{S}(\Omega) + \mathbf{D}_{\mathrm{mod}}\mathbf{P}(\Omega) + \mathbf{V})]^{-1}\mathbf{\Phi}_1^{\mathrm{rf}^{\mathrm{T}}}, \tag{27}$$

and hence

$$\mathbf{u}_1^{\mathrm{rf}}(\omega,\Omega) = \mathbf{H}_1^{\mathrm{rf}}(\omega,\Omega)\mathbf{F}_1(\omega). \tag{28}$$

Eq. (28) relates a force acting at any point on the tyre to the displacement at every point on the tyre. In order to calculate the vibrational response of a rolling tyre, the forces that arise from the tyre/road contact must be determined. Since the forces outside the contact area are zero, it is possible to solve the contact problem using only a small sub-matrix of $\mathbf{H}_1^{\mathrm{rf}}(\omega,\Omega)$ defined by those points of the tyre that are likely to come into contact with the road. However, the contact between the tyre and the road is of nonlinear nature and the description of the vibrational properties of the tyre should be formulated in the time-domain. One possibility is to perform an Inverse Fourier Transform on the sub-matrix of $\mathbf{H}_1^{\mathrm{rf}}(\omega,\Omega)$ to determine the Green's functions (impulse response) of the tyre. Then only this sub-matrix is needed to calculate the contact forces and the response of the whole tyre can be determined afterwards using the full matrix. Alternatively, Eq. (22) can be directly used to determine the response of the rotating tyre in the time-domain.

3.4. Discussion

It has been shown that reference frame-fixed modes should be used to model the behavior of a rotating tyre when a modal approach based on the natural frequencies and modeshapes of a loaded tyre is used. These modes are fixed in the reference frame, but rotate along with the excitation in the body-fixed frame. The approach presented in Section 3.3 has some interesting properties:

- A receptance matrix $\mathbf{H}_1^{\mathrm{rf}}(\omega, \Omega)$ can be defined for the rotating tyre. When calculating the response due to a roughness profile, only the points likely to come into contact with the road have to be taken into account. The total response can be calculated afterwards.
- A nonuniform mesh can be used, which makes it possible to model the contact area with a very fine mesh and use a coarser mesh for the rest of the tyre.
- The response in this reference frame can be used directly to calculate the resultant forces on the axle (responsible for the interior structureborne noise).
- A full 3D-contact model can be combined with the 3D-description of the tyre dynamic behavior in the proposed approach.

4. Results

To test the approach described in the previous section, two models are used. A 2D-ring model and a slightly more complex 3D model (see Fig. 3). In these models, a noncontact situation has been considered (both models are axisymmetric) in order to be able to compare the results to literature (mainly Ref. [13]).

For the ring models, 200 beam elements have been used (the figure shows a model with only 72 beam elements) in the FE calculation which resulted in a 600 dof model. In total, 100 modes have been used with frequencies up to 2000 Hz. The parameters of the ring model can be found in Table 1. For the 3D model, 3700 brick elements have been used, resulting in 7600 dofs. An inflation pressure of 10^6 Pa has been used, and 100 modes have been determined with frequencies up to ± 700 Hz. The parameters of the 3D model (Table 2) have been chosen to have the lower resonance frequencies in the same range as it is found for tyres. It should be noted that, although the above parameters models are not realistic for tyres, they suffice to illustrate the validity of the proposed methodology for the analysis of a rotating tyre.

4.1. 2D Ring model

To clarify the theory with the reference frame fixed modes from Section 3.3, an analytical description of the 2D-ring is used. It is wellknown (e.g., Ref. [24]) that the radial displacements of the modeshapes of a ring are $u_1 = \cos(n\alpha)$ and $u_2 = \sin(n\alpha)$. Here n is the number of waves along the circumference.

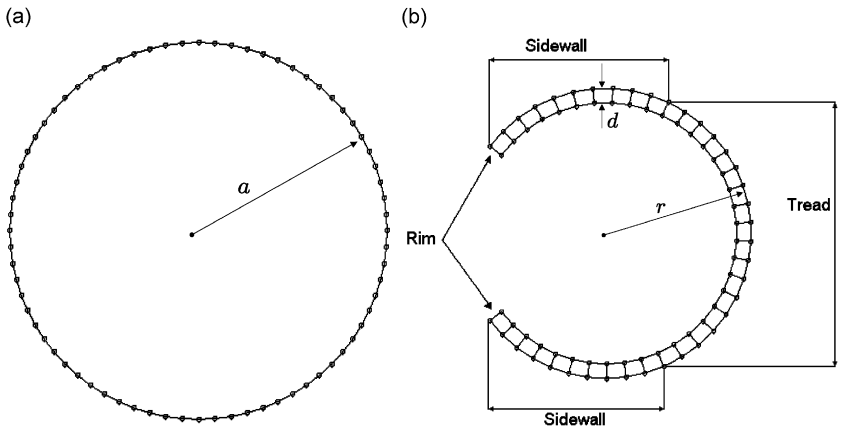

Fig. 3. (a) The FE model of the ring. Here shown with only 72-beam elements. (b) Cross-section 3D FE model.

Table 1
Parameters of the ring model

Parameter	Definition	Value
a	Radius of the ring	0.3 m
E	Elastic modulus of the ring material	$2 \cdot 10^9$ N/m^2
v	Poisson ratio of the ring material	0.3
ρ	Density of the ring material	7800 kg/m^3
r	Radius of the circular cross-section	0.005 m

Table 2
Parameters of the 3D model

Parameter	Definition	Value
a	Outer tyre radius	0.3 m
d	Tread/Sidewall thickness	0.01 m
E	Elastic modulus of the tread and sidewall material	$4.8 \cdot 10^8$ N/m^2
v	Poisson ratio of the tread and sidewall material	0.45
ρ	Density of the material	1200 kg/m^3
r	Outer radius of the circular cross-section	0.1 m

These analytical modeshapes are used to calculate the eigenvalues in the body-fixed frame and in the reference frame. In the body-fixed frame, the body-fixed modeshapes are written as

$$\mathbf{\Phi}_2^{\mathrm{bf}} = [\cos(n\alpha) \quad \sin(n\alpha)], \tag{29}$$

and the reference frame fixed modes $\mathbf{\Phi}_1^{\mathrm{rf}}$ are given by

$$\mathbf{\Phi}_1^{\mathrm{rf}} = [\cos(n\beta) \quad \sin(n\beta)]. \tag{30}$$

The diagonal matrix $\mathbf{V}$ in which the eigenfrequency is associated to these modeshapes is given by

$$\mathbf{V} = \begin{bmatrix} \omega_k^2 & 0 \\ 0 & \omega_k^2 \end{bmatrix}, \tag{31}$$

where ω_k is the eigenfrequency. We can now write the equations in state-space form and the eigenvalues in the fixed body frame can be determined by

$$\det(\lambda \mathbf{I} - \mathbf{B}_2^{\mathrm{bf}}) = 0, \tag{32}$$

where

$$\mathbf{B}_2^{\mathrm{bf}} = \begin{bmatrix} \mathbf{0} & \mathbf{I} \\ -\mathbf{V} & \mathbf{0} \end{bmatrix}. \tag{33}$$

This leads to the (trivial) eigenvalues: $\lambda = [\mathrm{i}\omega_k \quad \mathrm{i}\omega_k \quad -\mathrm{i}\omega_k \quad -\mathrm{i}\omega_k]$.

For the reference frame-fixed modes in Eulerian coordinates, the following set of equations can be found:

$$\ddot{\boldsymbol{\eta}}(t) + 2\Omega \begin{bmatrix} 0 & n \\ -n & 0 \end{bmatrix} \dot{\boldsymbol{\eta}}(t) + (\mathbf{V} - n^2\Omega^2\mathbf{I})\boldsymbol{\eta}(t) = \mathbf{\Phi}_1^{\mathrm{rf}\,\mathrm{T}} \mathbf{f}_1 \tag{34}$$

and the eigenvalues in the reference frame can be determined by

$$\det(\lambda \mathbf{I} - \mathbf{B}_1^{\mathrm{rf}}) = 0, \tag{35}$$

where

$$\mathbf{B}_1^{\mathrm{rf}} = \begin{bmatrix} \mathbf{0} & \mathbf{I} \\ n^2\Omega^2\mathbf{I} - \mathbf{V} & \begin{bmatrix} 0 & -2\Omega n \\ 2\Omega n & 0 \end{bmatrix} \end{bmatrix}. \tag{36}$$

Equation (35) leads to the following eigenvalues:

$$\lambda = [\mathrm{i}(\omega_k - n\Omega)\ \mathrm{i}(\omega_k + n\Omega)\ -\mathrm{i}(\omega_k - n\Omega)\ -\mathrm{i}(\omega_k + n\Omega)],$$

which clearly shows the splitting of the eigenvalues. Similar conclusions can be derived from the 2D-FE ring model. As discussed in Section 2, the rotation of the tyre leads to a shift of the dispersion curves. To show the splitting of the eigenvalues on the dispersion curves, the FRFs of all nodes on the ring in the radial direction are determined using Eq. (28) for a radial excitation at $\beta = 0$ in the frequency range 0–1000 Hz. The damping matrix is chosen by $\mathbf{D} = \alpha_R \mathbf{M}_1^{\mathrm{rf}}$ (Rayleigh damping), with $\alpha_R = 750\,\mathrm{s}^{-1}$. Subsequently, for each frequency for which the steady-state response is calculated, a spatial FFT is performed for the "upstream" ($\beta < 0$) half and the "downstream" ($\beta > 0$) half of the ring. This leads to the continuous dispersion plots shown in Fig. 4. The positive wave numbers correspond to waves travelling in the direction $\beta > 0$ and the negative wave numbers correspond to waves travelling in the direction $\beta < 0$. The triangular symbols in the figures indicate the eigenfrequencies determined in the eigenvalue analysis for $\Omega = 0$. The square symbols are the corrected eigenvalues using the equation of Kim and Bolton Eq. (1).

By comparison of Fig. 4(b) with Fig. 4(a), the asymmetry of the dispersion plots due to the tyre rotation can be clearly seen for frequencies above approximately 100 Hz. It is also clear that the tilting of the dispersion plots agrees with the prediction of the kinematic shift from Eq. (1). Below 100 Hz standing wave phenomena corresponding to the patterns of the lower three modes are observed. This behavior is not representative for the phenomenon of standing waves in real tyres, which occurs at higher rotational velocities and involves higher-order modes [25].

Figs. 5 and 6 show the FRF of the ring at selected frequencies (250 Hz, 500 Hz and 1000 Hz) for two different values of the rotational speed as a function of circumferential position (left) and wave number (right). The excitation force acts in the radial direction at $\beta = 0$, and the response is in the radial direction. As before, damping has been modelled as Rayleigh damping with $\alpha_R = 750\,\mathrm{s}^{-1}$. From Figs. 5(a) and 6(a), it can be concluded that the vibration levels are higher in the downstream direction (the positive circumferential

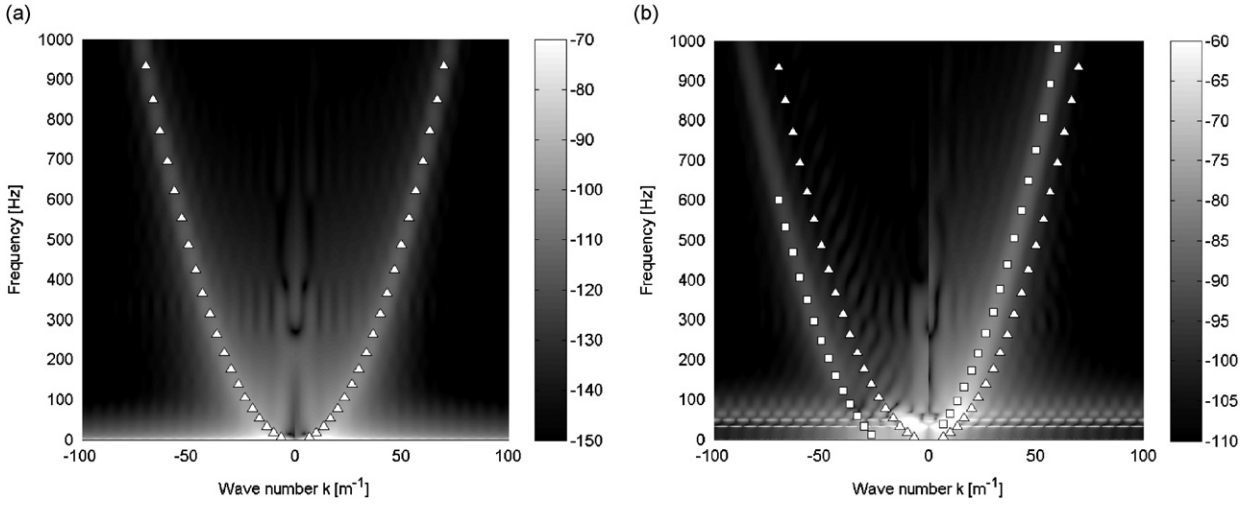

Fig. 4. Dispersion characteristics of the ring model for $\alpha_R = 750\,\mathrm{s}^{-1}$. (a) $\Omega = 0\,\mathrm{rad/s}$, (b) $\Omega = 100\,\mathrm{rad/s}$.

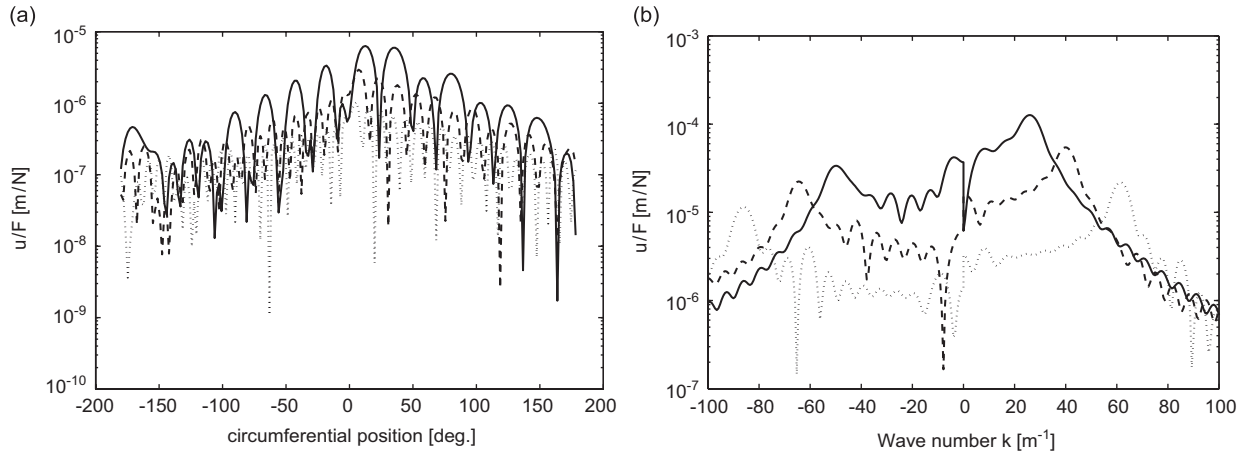

Fig. 5. Receptance for $\Omega = 100\,\text{rad/s}$ and $\alpha_R = 750\,\text{s}^{-1}$ at 250 Hz (solid), 500 Hz (dashed) and 1000 Hz (dotted). As a function of (a) circumferential position (deg), (b) wavenumber (m^{-1}).

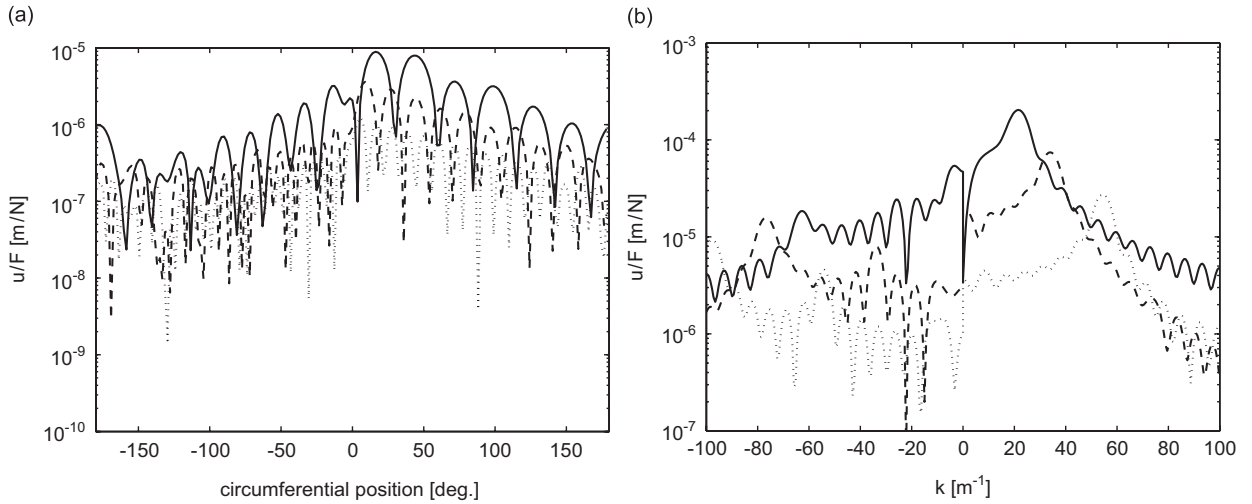

Fig. 6. Receptance for $\Omega = 175\,\text{rad/s}$ and $\alpha_R = 750\,\text{s}^{-1}$ at 250 Hz (solid), 500 Hz (dashed) and 1000 Hz (dotted). As a function of (a) circumferential position (deg), (b) wavenumber (m^{-1}).

positions) and this effect becomes clearer at higher rotational velocities. This result is in agreement with the observations made in Ref. [13]. However, it should be noted that this conclusion only applies to the simplified model studied here and not to tyres in general. It is well known [25] that if the speed of the waves propagating in the upstream direction coincides with the rotation velocity of the tyre, a standing wave pattern appears and the above conclusion is no longer valid.

It is interesting to observe the FRF as a function of the wave number in Figs. 5(b) and 6(b), where positive wave numbers represent waves travelling "downstream" ($\beta > 0$), and negative wave numbers represent waves travelling "upstream" ($\beta < 0$). The vibration field is dominated by two main waves having different wavenumbers and opposite signs (therefore travelling in opposite directions). This means that these two waves form a vibration pattern which is rotating. A similar result can be found in Ref. [10]. However, unlike in Ref. [10], the peaks corresponding to these dominant waves are still clearly visible for higher frequencies, which is due to the type of damping chosen for the ring model. For more realistic tyre parameters, it has been shown that the peaks become less sharp as frequency increases [10].

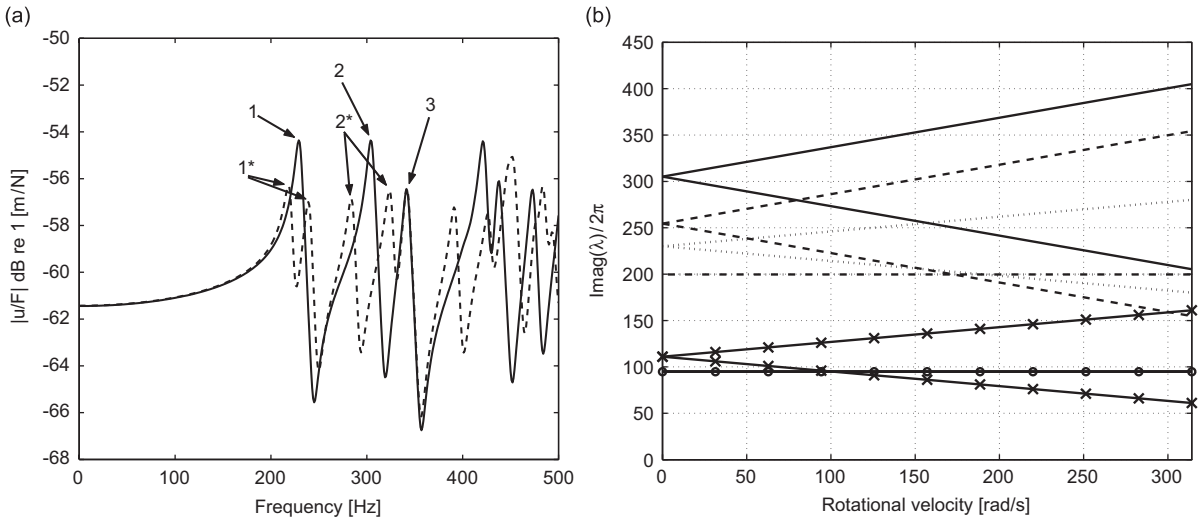

Fig. 7. (a) Radial point admittance of the 3D model for $\Omega = 0$ rad/s (solid line) and $\Omega = 20\pi$ rad/s (dashed line). (b) Eigenvalues of the first 10 modes for different Ω's.

4.2. Simplified 3D-tyre model

In the previous sections, the theory from Section 3.3 has been verified using a 2D-ring model. In this section, it is shown that for the 3D model, the splitting of frequencies is also correctly modelled.

Fig. 7(a) shows the point admittance in the radial direction at a point on the middle circle of the 3D model for rotational velocities of 0 and 20π rad/s. In the figure, index 1 denotes a mode with $n = 1$. Index 1^* denotes the two modes which appear when the tyre is rotating. These modes are shifted $\pm 20\pi/2\pi = \pm 10$ Hz with respect to the non-rotating situation. Indices 2 and 2^* denote modes with $n = 2$ for the nonrotating and rotating tyre, respectively. The latter are shifted $\pm 2\ 20\pi/2\pi \approx \pm 20$ Hz. Index 3 denotes a modeshape with $n = 0$. The frequency of this mode does not shift as a result of rotation as there is no variation of this modeshape along the circumference. The effect of rotation on the eigenfrequencies of the tyre is also shown in Fig. 7(b). In this figure the eigenvalues corresponding to the 10 first eigenmodes are shown. Again the splitting of the eigenvalues can be seen. The slope of the lines is determined by the number of wavelengths along the circumference (or the wave number k_ϕ), which is in agreement with Eq. (1).

5. Conclusions

This paper examines an approach to model the vibrations of deformed rotating tyres in the lower frequency range. Determining the eigenvalues and eigenmodes of a detailed FE-model of the tyre and then using these to construct a modal base of the tyre seems a computationally efficient way of calculating the dynamic response of the tyre taking its complex build-up into account. The presented methodology allows for the calculation of the response of the rotating tyre in a fixed (Eulerian) reference frame, including the influence of gyroscopic and centrifugal forces.

In the approach proposed here, the large deformations due to the stationary tyre loading and the small-scale vibrations originated by the tyre/road interaction are treated separately. This enables the determination of the large stationary deformations with the full equations and possibly nonlinear material properties, while the small, transient displacements are superposed on this state in a linear sense by using a limited number of modes. In this way, the natural frequencies and modeshapes of a deformed tyre can be determined in any standard FE package using the full model. Using the modal base thus acquired, the response of the rotating tyre can be found by applying a coordinate transformation and a transfer function can be calculated from a force at any point in the contact patch to the response at any point on the tyre (or to the force transmitted to

the axle). Furthermore, the presented approach can be combined with a full 3D-contact model, which will be the subject of future research.

The modelling approach presented in this paper has some drawbacks:

- A good FE model of a tyre is needed.
- In Eq. (23) and (24) the full mass matrix of the FE model is used. For a large model, exporting the mass matrix and computing **P** and **S** using Eq. (23) and (24) could be a serious problem. However, it should be kept in mind that these matrices only have to be computed once and that their final size is equal to the number of modes chosen.

The proposed methodology has been applied to two relatively simple models showing that the effects of rotation are modelled correctly and are in accordance with results from the literature.

Appendix A. System equations including damping

To be able to include damping in the new approach, a damping matrix $\mathbf{D}_1^{\mathrm{rf}}$ of dimensions ($ndof * ndof$) is required. When using proportional damping, this matrix can be determined from $\mathbf{D}_{\mathrm{mod}}$ by using the following identities:

$$\mathbf{\Phi}_1^{\mathrm{rf}\,\mathrm{T}}\mathbf{M}_1^{\mathrm{rf}}\mathbf{\Phi}_1^{\mathrm{rf}} = \mathbf{I} \tag{A.1}$$

$$\mathbf{\Phi}_1^{\mathrm{rf}\,\mathrm{T}}\mathbf{D}_1^{\mathrm{rf}}\mathbf{\Phi}_1^{\mathrm{rf}} = \mathbf{D}_{\mathrm{mod}}. \tag{A.2}$$

The above equations can be used to write

$$\mathbf{\Phi}_1^{\mathrm{rf}\,\mathrm{T}}\mathbf{D}_1^{\mathrm{rf}}\mathbf{\Phi}_1^{\mathrm{rf}} = \mathbf{\Phi}_1^{\mathrm{rf}\,\mathrm{T}}\mathbf{M}_1^{\mathrm{rf}}\mathbf{\Phi}_1^{\mathrm{rf}}\mathbf{D}_{\mathrm{mod}}\mathbf{\Phi}_1^{\mathrm{rf}\,\mathrm{T}}\mathbf{M}_1^{\mathrm{rf}}\mathbf{\Phi}_1^{\mathrm{rf}}, \tag{A.3}$$

which means that

$$\mathbf{D}_1^{\mathrm{rf}} = \mathbf{M}_1^{\mathrm{rf}}\mathbf{\Phi}_1^{\mathrm{rf}}\mathbf{D}_{\mathrm{mod}}\mathbf{\Phi}_1^{\mathrm{rf}\,\mathrm{T}}\mathbf{M}_1^{\mathrm{rf}}. \tag{A.4}$$

Including $\mathbf{D}_2^{\mathrm{rf}}\dot{\mathbf{u}}_2(\beta, t)$ in Eq. (19) and transforming to eulerian coordinates with Eq. (20) leads to (the derivation is only shown for the extra damping term in Eq. (19))

$$\mathbf{D}_2^{\mathrm{rf}}\frac{\mathrm{D}\dot{\mathbf{u}}_2(\beta t, t)}{\mathrm{D}t} = \mathbf{D}_2^{\mathrm{rf}}\left(\frac{\partial\dot{\mathbf{u}}_2(\beta t, t)}{\partial t} + \Omega\frac{\partial\dot{\mathbf{u}}_2(\beta t, t)}{\partial\beta}\right), \tag{A.5}$$

which after transforming back to reference coordinates and pre-multiplying with $\mathbf{\Phi}_1^{\mathrm{rf}\,\mathrm{T}}$ leads to

$$\mathbf{\Phi}_1^{\mathrm{rf}\,\mathrm{T}}\mathbf{D}_1^{\mathrm{rf}}\mathbf{\Phi}_1^{\mathrm{rf}}\dot{\boldsymbol{\eta}}(t) + \mathbf{\Phi}_1^{\mathrm{rf}\,\mathrm{T}}\mathbf{D}_1^{\mathrm{rf}}\left(\hat{\mathbf{\Omega}}\mathbf{\Phi}_1^{\mathrm{rf}}(\beta) + \Omega\frac{\partial\mathbf{\Phi}_1^{\mathrm{rf}}(\beta)}{\partial\beta}\right)\boldsymbol{\eta}(t). \tag{A.6}$$

Finally, by using Eq. (23), Eq. (A.1) and Eq. (A.4) the above equation can be written as

$$\mathbf{D}_{\mathrm{mod}}\dot{\boldsymbol{\eta}}(t) + \mathbf{D}_{\mathrm{mod}}\mathbf{P}(\Omega)\boldsymbol{\eta}(t), \tag{A.7}$$

leading to the following full equations including modal damping:

$$\ddot{\boldsymbol{\eta}}(t) + (2\mathbf{P}(\Omega) + \mathbf{D}_{\mathrm{mod}})\dot{\boldsymbol{\eta}}(t) + (\mathbf{S}(\Omega) + \mathbf{D}_{\mathrm{mod}}\mathbf{P}(\Omega) + \mathbf{V})\boldsymbol{\eta}(t) = \mathbf{\Phi}_1^{\mathrm{rf}\,\mathrm{T}}(\beta)\mathbf{f}_1(t). \tag{A.8}$$

Therefore, proportional damping can be included in this approach with little extra computational cost, since $\mathbf{P}(\Omega)$ has already been calculated and $\mathbf{D}_{\mathrm{mod}}$ can easily be constructed from the modal damping ratios and eigenfrequencies.

References

[1] U. Sandberg, Tyre/road noise—Myths and realities, *Proceedings of Inter-noise 2001*, 2001.
[2] U. Sandberg, J.A. Ejsmont, *Tyre/road Noise Reference Book*. Informex, SE-59040 Kisa, Sweden, 2002.

[3] W. Kropp, K. Larsson, F. Wullens, P. Andersson, F.X. Becot, The generation of tyre/road noise—mechanisms and models, ICSV 10, 2003.
[4] M. Heckl, Tyre noise generation, *Wear* 113 (1986) 157–170.
[5] W. Kropp, Structure-borne sound on a smooth tyre, *Applied Acoustics* 26 (1989) 181–192.
[6] S. Gong, A Study of In-plane Dynamics of Tires. PhD Thesis, Delft University of Technology, Faculty of mechanical engineering and marine technology, 1993.
[7] W. Kropp, A mathematical model of tyre noise generation, *Heavy Vehicle Systems, International Journal of Vehicle Design* 6 (1–4) (1999) 310–329.
[8] K. Larsson, W. Kropp, A high-frequency three-dimensional tyre model based on two coupled elastic layers, *Journal of Sound and Vibration* 253 (4) (2002) 889–908.
[9] J.M. Muggleton, B.R. Mace, M.J. Brennan, Vibrational response prediction of a pneumatic tyre using an orthotropic two-plate wave model, *Journal of Sound and Vibration* 254 (2003) 929–950.
[10] F. Wullens, W. Kropp, Wave content of the vibration field of a rolling tyre, *Acta Acustica United with Acustica* 293 (1) (2007) 48–56.
[11] W. Soedel, On the dynamic response of rolling tires according to thin shell approximations, *Journal of Sound and Vibration* 41 (1975) 233–246.
[12] R.F. Keltie, Analytical model of the truck tyre vibration sound mechanism, *Journal of the Acoustical Society of America* 71 (2) (1982) 359–367.
[13] Y.J. Kim, J.S. Bolton, Effects of rotation on the dynamics of a circular cylindrical shell with applications to tire vibration, *Journal of Sound and Vibration* 275 (3–5) (2003) 605–621.
[14] R.J. Pinnington, A wave model of a circular tyre. Part 1: belt modelling, *Journal of Sound and Vibration* 290 (1–2) (2006) 101–132.
[15] R.J. Pinnington, A wave model of a circular tyre. Part 2: side-wall and force transmission modelling, *Journal of Sound and Vibration* 290 (1–2) (2006) 133–168.
[16] C.M. Nilsson, Waveguide Finite Elements Applied on a Car Tyre, Doctoral Thesis, KTH, Aeronautics and Vehicle Engineering, ISBN 91-7283-798-5, 2004.
[17] Y.B. Chang, T.Y. Yang, W. Soedel, Dynamic analysis of a radial tire by finite elements and modal expansion, *Journal of Sound and Vibration* 96 (1) (1984) 1–11.
[18] D.J. Thompson, Wheel-rail noise generation, part V: inclusion of wheel rotation, *Journal of Sound and Vibration: inclusion of wheel rotation* 161 (3) (1993) 467–482 *Inter-noise 2004*, 2004.
[19] M. Brinkmeier, U. Nackenhorst, O. von Estorff, S. Petersen, Physically based modelling of tire-rolling-noise by a finite element approach, Inter-noise 2004, 2004.
[20] U. Nackenhorst, The ALE-formulation of bodies in rolling contact: theoretical foundations and finite element approach, *Computer Methods in Applied Mechanics and Engineering* 193 (39–41) (2004) 4299–4322.
[21] J. Padovan, Natural frequencies of rotating prestressed cylinders, *Journal of Sound and Vibration* 31 (4) (1973) 469–482.
[22] S.C. Huang, W. Soedel, Effects of coriolis acceleration on the free and forced in-plane vibrations of rotating rings on elastic foundation, *Journal of Sound and Vibration* 115 (2) (1987) 253–274.
[23] D.S. Stutts, W. Soedel, A simplified dynamic model of the effect of internal damping on the rolling resistance in pneumatic tires, *Journal of Sound and Vibration* 155 (1) (1992) 153–164.
[24] R.D. Blevins, *Formulas for Natural Frequency and Mode Shape*, Van Nostrand Reinhold, London, 1979.
[25] J. Padovan, On standing waves in tires, *Tire Science and Technology* 5 (1977) 83–101.